Search methods for tile sets in patterned DNA self-assembly[☆]

Mika Göös[1], Tuomo Lempiäinen[1], Eugen Czeizler[2,*], Pekka Orponen[2]

Department of Information and Computer Science and
Helsinki Institute for Information Technology HIIT
Aalto University, Finland

Abstract

The Pattern self-Assembly Tile set Synthesis (PATS) problem, which arises in the theory of structured DNA self-assembly, is to determine a set of coloured tiles that, starting from a bordering seed structure, self-assembles to a given rectangular colour pattern. The task of finding minimum-size tile sets is known to be NP-hard. We explore several complete and incomplete search techniques for finding minimal, or at least small, tile sets and also assess the reliability of the solutions obtained according to Winfree's kinetic Tile Assembly Model.

Keywords: DNA self-assembly, tilings, Tile Assembly Model, pattern assembly, tile set synthesis, reliable self-assembly

1. Introduction

Algorithmic assembly of nucleic acids (DNA and RNA) has advanced extensively in the past 30 years, from a seminal idea to the current designs and experimental implementations of complex nanostructures and nanodevices with dynamic programmable evolution and machinelike properties. Recent developments in the field include in vitro complex 3D patter formation and functionalisation [4, 10], robotic constructions such as mobile arms, walkers, motors [18, 33], computational primitives [22, 23], but also in vivo biosensors [14] and potential drug delivery mechanisms and therapeutics [12].

Self-assembly of nucleic acids can be seen both as a form of structural nanotechnology and as a model of computation. As a computational model, one first encodes the input of a computational problem into an algorithmically designed

[☆]Preliminary versions of parts of this work have appeared in the *Proceedings of the 16th* and *17th International Conference on DNA Computing and Molecular Programming* (Hong Kong, China, June 2010, and Pasadena, CA, Sept. 2011, respectively) [8, 11].

[*]Corresponding author.

[1]Current affiliation: Helsinki Institute for Information Technology HIIT, and Department of Computer Science, University of Helsinki. Email addresses: firstname.lastname@helsinki.fi.

[2]Email addresses: firstname.lastname@aalto.fi.

(DNA) pattern or shape. Then, by making use of both the initial oligomer design and the intrinsic properties of the self-assembly system, one manipulates the structure to produce a new architecture that encodes the desired output.

As a nanotechnology, the goal of algorithmic (DNA/RNA) self-assembly is to design oligomer sequences that in solution would autonomously (or with as little interaction as possible) assemble into complex polymer structures. These may have both static and dynamic properties, may bind other molecules such as gold nanoparticles or various proteins, may act as fully addressable scaffolds, or may be used for further manipulation. Such molecular constructions can consist from only a couple of DNA strands to more than 200 and, in some cases, can change their conformation and achieve distinct functionalities.

In recent years there has been a growing interest in integrating these two directions, in order to obtain complex supramolecular constructions with interdependencies between computational functions and conformational switching. Such approaches are envisioned due to a key property of nucleic acid scaffolds, viz. their modularity: multiple functional units can be attached to a common scaffold, thus giving rise to multifunctional devices. Thus, the self-assembly of nanostructures templated on synthetic DNA has been proposed by several authors as a potentially ground-breaking technology for the manufacture of next-generation circuits, devices, and materials [9, 20, 31, 32]. Also laboratory techniques for synthesizing the requisite 2D DNA template lattices, many based on Rothemund's [25] DNA origami tiles, have recently been demonstrated by many groups [15, 24].

In order to support the manufacture of aperiodic structures, such as electronic circuit designs, these DNA templates need to be addressable. When the template is constructed as a tiling from a family of DNA origami (or other kinds of) tiles, one can view the base tiles as being "coloured" according to their different functionalities, and the completed template implementing a desired colour pattern[3]. Now, a given target pattern can be assembled from many different families of base tiles, and to improve the laboratory synthesis it is advantageous to try to minimise the number of tile types needed and/or maximise the probability that they self-assemble to the desired pattern, given some characteristics of the tiling errors.

The task of minimising the number of DNA tile types required to implement a given 2D pattern was identified by Ma and Lombardi [19], who formulated it as a combinatorial optimisation problem, the *Pattern self-Assembly Tile set Synthesis* (PATS) problem, and also proposed two greedy heuristic algorithms for solving the task. The problem was recently proved to be NP-hard [3, 28], and hence finding an absolutely minimum size tile set for a given pattern most likely requires an exponential amount of time in the worst case. Thus the problem needs to be addressed either with complete methods yielding optimal tile sets for small patterns, or incomplete methods that work also for larger patterns but do

[3]For an example of such a tile-based high-level design scheme for nano-electric circuits please read the attached Supplementary Information, detailing the results from [2].

not guarantee that the tile sets produced are of minimal size. In this work, we present search algorithms covering both approaches and assess their behaviour experimentally using both randomly generated and benchmark pattern test sets. We attend both to the running times of the respective algorithms, and to the size and assembly reliability of the tile sets produced.

In the following, we first in Section 2 present an overview of the underlying Tile Assembly Model [30, 26] and the PATS problem [19], and then in Section 3 discuss the search space of pattern-consistent tile sets (viewed abstractly as partitions of the ambient rectangular grid). In Section 4 we proceed to describe our exhaustive partition-search branch-and-bound algorithm (PS-BB) to find tile sets of absolutely minimum cardinality. The algorithm makes use of a search tree in the lattice of grid partitions, and an efficient bounding function to prune this search tree.

While the PS-BB algorithm can be used to find certifiably minimal tile sets for small patterns, the size of the search space grows so rapidly that the algorithm hits a complexity barrier at approximately pattern sizes of 7×7 tiles, for random test patterns. Thus, in a second approach, presented in Section 5, we tailor the basic partition-search framework of the PS-BB algorithm towards the goal of finding small, but not necessarily minimal tile sets. Instead of a systematic branch-and-bound pruning and traversal of the complete search space, the modified algorithm PS-H applies heuristics which attempt to optimise the order of the directions in which the space is explored.

It is well known in the heuristic optimisation community [7, 16] that when the runtime distribution of a randomised search algorithm has a large variance, it is with high probability more efficient to run several independent short runs ("restarts") of the algorithm than a single long run. Correspondingly, we investigate the efficiency of the PS-H algorithm for a number of parallel executions ranging from 1 to 32, and note that indeed this number has a significant effect on the success rate of the algorithm in finding small tile sets.

As a third alternative, presented in Section 6, we formulate the PATS problem as an Answer Set Programming (ASP) task [13], and apply generic ASP solvers to find solutions to it. Here our experimental results indicate that for patterns with a known small minimal solution, the ASP approach indeed works well in discovering that solution.

Given the inherently stochastic nature of the DNA self-assembly process, it is important also to assess the reliability of a given tile set, i.e. the probability of its error-free self-assembly to the desired target pattern. In Section 7 we introduce a method for estimating this quantity, based on Winfree's analysis of the kinetic Tile Assembly Model [30]. We present experimental data on the reliability of tile sets found by the PS-BB and PS-H algorithms and find that also here the heuristic optimisations introduced in the PS-H approach result in a notable improvement over the basic PS-BB method.

2. Preliminaries

In this section, we first briefly review the abstract Tile Assembly Model (aTAM) from [30, 26] and summarize the PATS problem from [19].

2.1. The Abstract Tile Assembly Model [26, 30]

The aTAM is a generalization of Wang tile systems, customary designed for the study of self-assembly systems. The basic components of the aTAM are non-rotatable unit square tiles, uniquely defined by the sets of four glues placed on top of their edges. The glues are part of a finite alphabet and each pair of glues is associated a strength value, determining the stability of a linked between two tiles having these glues on the abutting edges. In most cases, it is assumed that the strength of two distinct glues is zero, while a pair of matching glues has strength either 1 or 2.

Let $\mathcal{D} = \{N, E, S, W\}$ be the set of four functions $\mathbb{Z}^2 \to \mathbb{Z}^2$ corresponding to the four cardinal directions. Let Σ be a finite set of *glue types* and $s : \Sigma \times \Sigma \to \mathbb{N}$ a *glue strength* function such that, unless otherwise specified, $s(\sigma, \sigma') > 0$ only if $\sigma = \sigma'$. A *tile type* $t \in \Sigma^4$ is a quadruple $(\sigma_N(t), \sigma_E(t), \sigma_S(t), \sigma_W(t))$ of glue types for each side of the unit square. A *tile system* $T \subseteq \Sigma^4$ is a finite collection of different tile types.

Given a tile system T, an *(tile) assembly* $\mathcal{A}$ is a partial mapping $\mathcal{A} : \mathbb{Z}^2 \to T$ assigning tiles to various elements from the two dimensional space. A *tile assembly system* (TAS) $\mathscr{T} = (T, \mathcal{S}, s, \tau)$ consists of a tile system T, a *seed assembly* $\mathcal{S}$, a glue strength function s and a *temperature* $\tau \in \mathbb{Z}^+$ (we use $\tau = 2$). Given an existing assembly $\mathcal{A}$, such as the seed structure $\mathcal{S}$, a tile can adjoin the assembly if the total strength of the binding, given by the sum of all strength functions among the glues placed on the boundary between the tile and the assembly, surpasses the temperature threshold τ.

Formally, we say that assembly $\mathcal{A}$ *produces directly* assembly $\mathcal{A}'$, denoted $\mathcal{A} \to_{\mathscr{T}} \mathcal{A}'$, if there exists a site $(x, y) \in \mathbb{Z}^2$ and a tile $t \in T$ such that $\mathcal{A}' = \mathcal{A} \cup \{((x, y), t)\}$, where the union is disjoint, and

$$\sum_{D} s(\sigma_D(t), \sigma_{D^{-1}}(\mathcal{A}(D(x, y)))) \;\geq\; \tau \;,$$

where D ranges over those directions in $\mathcal{D}$ for which $\mathcal{A}(D(x, y))$ is defined.

In Figure 1 we present a TAS with seven tile types and temperature $\tau = 2$ which, starting from the seed tile, assembles a continuously growing structure corresponding to the Binary Counter pattern. Out of the seven tile types in Figure 1 a), one can distinguish the tile **s** used as seed, two tile types which assemble the boundary of the structure, and four rule-tile types, which fill the area in between the "V" shaped boundary.

Let $\to^*_{\mathscr{T}}$ be the reflexive transitive closure of $\to_{\mathscr{T}}$. A TAS $\mathscr{T}$ *produces* an assembly $\mathcal{A}$ if $\mathcal{A}$ is an extension of the seed assembly $\mathcal{S}$, that is $\mathcal{S} \to^*_{\mathscr{T}} \mathcal{A}$. Denote by Prod $\mathscr{T}$ the set of all assemblies produced by $\mathscr{T}$. A TAS $\mathscr{T}$ is *deterministic* if for any assembly $\mathcal{A} \in$ Prod $\mathscr{T}$ and for every $(x, y) \in \mathbb{Z}^2$ there exists at most

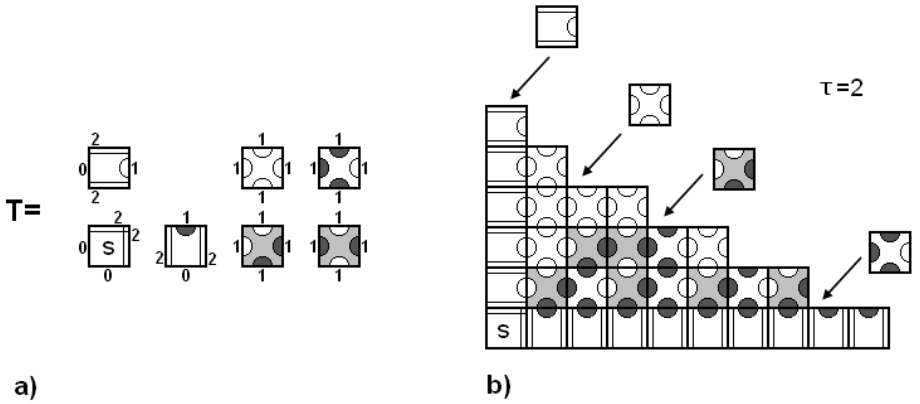

Figure 1: (a) The Binary Counter tile set; the different glues are graphically differentiated, while their associated strengths are marked accordingly. The colour of the tiles is an indicator of which tiles represent a black/white spot in the pattern.(b) The assembly of the Binary Counter pattern for a TAS using the tile set T, the seed structure **s**, and the temperature threshold τ.

one $t \in T$ such that $\mathcal{A}$ can be extended with t at site (x, y). Then the pair $(\text{Prod}\,\mathscr{T}, \to^*_{\mathscr{T}})$ forms a partially ordered set, which is a lattice if and only if $\mathscr{T}$ is deterministic. The maximal elements in $\text{Prod}\,\mathscr{T}$, i.e. the assemblies $\mathcal{A}$ for which there do not exist any $\mathcal{A}'$ satisfying $\mathcal{A} \to_{\mathscr{T}} \mathcal{A}'$, are called *terminal assemblies*. Denote by $\text{Term}\,\mathscr{T}$ the set of terminal assemblies of $\mathscr{T}$. In case of finite assemblies, an equivalent definition of determinism is that all *assembly sequences* $\mathcal{S} \to_{\mathcal{T}} \mathcal{A}_1 \to_{\mathcal{T}} \mathcal{A}_2 \to_{\mathcal{T}} \cdots$ terminate and $\text{Term}\,\mathcal{T} = \{\mathcal{P}\}$ for some assembly $\mathcal{P}$. In this case we say that $\mathcal{T}$ *uniquely produces* $\mathcal{P}$.

2.2. The PATS Problem

Let the dimensions m and n be fixed. A mapping from $[m] \times [n] \subseteq \mathbb{Z}^2$ onto $[k]$ defines a *k-colouring* or a *k-coloured pattern*. To build a given pattern, we start with boundary tiles in place for the west and south borders of the m by n rectangle and keep extending this assembly by tiles with strength-1 glues.

Definition 1 (Pattern self-Assembly Tile set Synthesis (PATS) [19])**.**

Given: *A k-colouring $c : [m] \times [n] \to [k]$.*
Find: *A tile assembly system $\mathscr{T} = (T, \mathcal{S}, s, 2)$ such that*

P1. *The tiles in T have glue strength 1.*

P2. *The domain of $\mathcal{S}$ is $[0, m] \times \{0\} \cup \{0\} \times [0, n]$ and all the terminal assemblies have domain $[0, m] \times [0, n]$.*

P3. *There exists a tile colouring $d : T \to [k]$ such that each terminal assembly $\mathcal{A} \in \text{Term}\,\mathscr{T}$ satisfies $d(\mathcal{A}(x, y)) = c(x, y)$ for all $(x, y) \in [m] \times [n]$.*

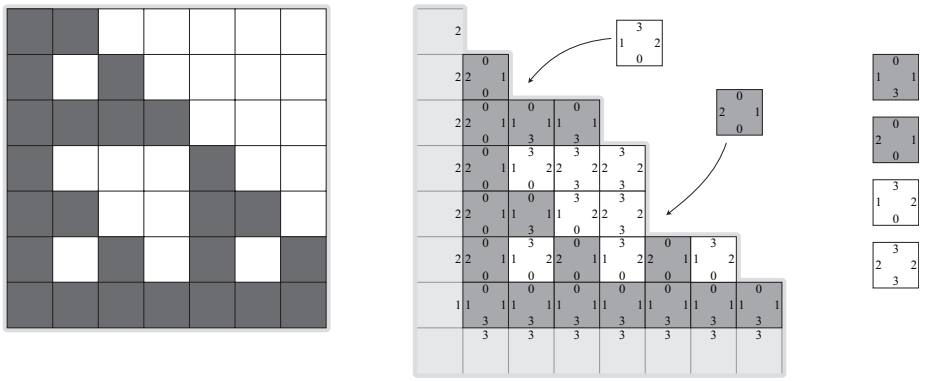

(a) (b) (c)

Figure 2: (a) A finite subset of the discrete Sierpinski triangle. This 2-colouring of the set $[7] \times [7]$ defines an instance of the PATS problem. (b) Assembling the Sierpinski pattern with a TAS that has an appropriate seed assembly and a (coloured) tile set shown in (c).

Finding minimal solutions (in terms of $|T|$) to the PATS problem has been claimed to be NP-hard in [19] and proved to be so in [3].[4] Without loss of generality, we consider only TASs $\mathscr{T}$ in which every tile type participates in some terminal assembly of $\mathscr{T}$.

As an illustration, In Fig. 2 we construct a 7×7 Sierpinski pattern starting from a 4-tile TAS. We use natural numbers as glue labels in our figures.

In the literature, the seed assembly of a TAS is often taken to be a single seed tile [26] whereas we consider an L-shaped seed assembly. The boundaries can always be self-assembled using $m+n+1$ different tiles with strength-2 glues, but we wish to make a clear distinction between the complexity of constructing the boundaries and the complexity of the 2D pattern itself. Moreover, in some experimental implementations of DNA tile assembly systems, e.g. [5], the seed structures are implemented using the DNA origami technique [25], which allows for the creation of such complete boundary conditions.

Due to constraint *P1* the self-assembly process proceeds in a uniform manner directed from south-west to north-east. This paves the way for a simple characterisation of deterministic TASs in the context of the PATS problem.

Proposition 1. *Solutions $\mathscr{T} = (T, \mathcal{S}, s, 2)$ of the PATS problem are deterministic precisely when for each pair of glue types $(\sigma_1, \sigma_2) \in \Sigma^2$ there is at most one tile type $t \in T$ so that $\sigma_S(t) = \sigma_1$ and $\sigma_W(t) = \sigma_2$.*

A simple observation reduces the work needed in finding minimal solutions of the PATS problem.

Lemma 2. *The minimal solutions of the PATS problem are deterministic TASs.*

[4] An improvement of the result to use only a constant number of tile colours is presented in [28].

Proof. For the sake of contradiction, suppose that $\mathscr{N} = (T, \mathcal{S}, s, 2)$ is a minimal solution to a PATS problem instance and that $\mathscr{N}$ is not deterministic. By the above proposition let tiles $t_1, t_2 \in T$ be such that $\sigma_S(t_1) = \sigma_S(t_2)$ and $\sigma_W(t_1) = \sigma_W(t_2)$. Consider the simplified TAS $\mathscr{N}' = (T \setminus \{t_2\}, \mathcal{S}, s, 2)$. We show that this, too, is a solution to the PATS problem, which violates the minimality of $|T|$.

Suppose $\mathcal{A} \in \operatorname{Term}\mathscr{N}'$. If $\mathcal{A} \notin \operatorname{Term}\mathscr{N}$, then some $t \in T$ can be used to extend $\mathcal{A}$ in $\mathscr{N}$. If $t \in T \setminus \{t_2\}$, then t could be used to extend $\mathcal{A}$ in $\mathscr{N}'$, so we must have $t = t_2$. But since new tiles are always attached by binding to south and west sides of the tile, $\mathcal{A}$ could then be extended by t_1 in $\mathscr{N}'$. Thus, we conclude that $\mathcal{A} \in \operatorname{Term}\mathscr{N}$ and furthermore $\operatorname{Term}\mathscr{N}' \subseteq \operatorname{Term}\mathscr{N}$. This demonstrates that $\mathscr{N}'$ has property *P2*. The properties *P1* and *P3* can be readily seen to hold for $\mathscr{N}'$ as well. In terms of $|T|$ we have found a more optimal solution—and a contradiction. □

We consider only deterministic TASs in the sequel.

3. The search space of consistent tile sets

Let X be the set of partitions of the set $[m] \times [n]$. Partition P is *coarser* than partition P' (or P' is a *refinement* of P), denoted $P \sqsubseteq P'$, if

$$\forall p' \in P' : \ \exists p \in P : \ p' \subseteq p \ .$$

Now, $(X, \sqsubseteq)$ is a partially ordered set, and in fact, a lattice. Note that $P \sqsubseteq P'$ implies $|P| \leq |P'|$.

The colouring c induces a partition $P(c) = \{c^{-1}(i) \mid i \in [k]\}$ of the set $[m] \times [n]$. In addition, since every (deterministic) solution $\mathscr{T} = (T, \mathcal{S}, s, 2)$ of the PATS problem uniquely produces some assembly $\mathcal{A}$, we associate with $\mathscr{T}$ a partition $P(\mathscr{T}) = \{\mathcal{A}^{-1}(t) \mid t \in \mathcal{A}([m] \times [n])\}$. Here, $|P(\mathscr{T})| = |T|$ in case all tiles in T are used in the terminal assembly. Now the condition *P3* in the definition of PATS is equivalent to requiring that a TAS $\mathscr{T}$ satisfies

$$P(c) \sqsubseteq P(\mathscr{T}) \ .$$

A partition $P \in X$ is *constructible* if $P = P(\mathscr{T})$ for some deterministic TAS $\mathscr{T}$ with properties *P1* and *P2*. Hence the PATS problem can be rephrased using partitions as the fundamental search space.

Proposition 3. *A minimal solution to the PATS problem corresponds to a partition $P \in X$ such that P is constructible, $P(c) \sqsubseteq P$, and $|P|$ is minimal.*

For example, the 2-coloured pattern in Fig. 3(a) defines a 2-part partition A. The 7-part partition M in Fig. 3(b) is a refinement of A ($A \sqsubseteq M$) and in fact, M is constructible (see Fig. 4(b)) and corresponds to a minimal solution of the PATS problem defined by the pattern A.

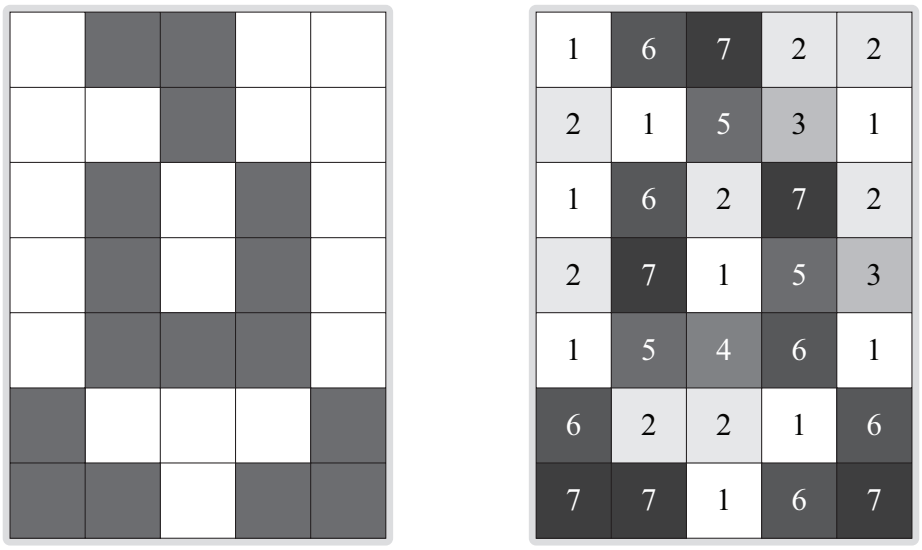

Figure 3: (a) Partition A. (b) A partition M that is a refinement of A with $|M| = 7$ parts.

3.1. Determining constructibility

In this section we give an algorithm for deciding the constructibility of a given partition in polynomial time. To do this, we use the concept of *most general* (or least constraining) *tile assignments*. For simplicity, we assume the set of glue labels Σ to be infinite.

Definition 2. *Given a partition P of the set $[m] \times [n]$, a* most general tile assignment *(MGTA) is a function $f : P \to \Sigma^4$ such that*

A1. When every position in $[m] \times [n]$ is assigned a tile type according to f, any two adjacent positions agree on the glue type of the side between them.

A2. For all assignments $g : P \to \Sigma^4$ satisfying A1 we have[5]

$$f(p_1)_{D_1} = f(p_2)_{D_2} \quad \Longrightarrow \quad g(p_1)_{D_1} = g(p_2)_{D_2} \tag{1}$$

for all $(p_1, D_1), (p_2, D_2) \in P \times \mathcal{D}$.

To demonstrate this concept we present a most general tile assignment $f : I \to \Sigma^4$ for the *initial partition* $I = \{\{a\} \mid a \in [m] \times [n]\}$ in Figure 4(a) and a MGTA for the partition of Figure 3(b) in Figure 4(b).

[5]To shorten the notation we write $f(p)_D$ instead of $\sigma_D(f(p))$.

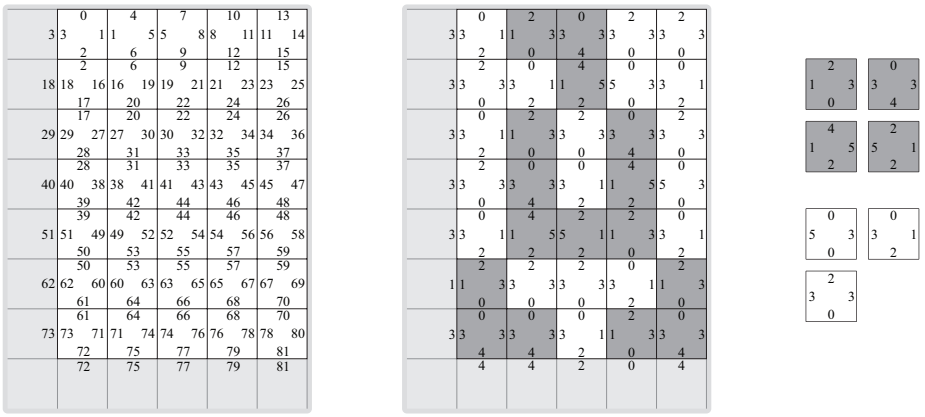

(a) (b) (c)

Figure 4: (a) A MGTA for the constructible initial partition I (with a seed assembly in place). (b) Finished assembly for the pattern from Figure 3a. The tile set to construct this assembly is given in (c).

Given a partition $P \in X$ and a function $f : P \to \Sigma^4$, we say that $g : P \to \Sigma^4$ is obtained from f by *merging glues a and b* if for all $(p, D) \in P \times \mathcal{D}$ we have

$$g(p)_D = \begin{cases} a, & \text{if } f(p)_D = b \\ f(p)_D, & \text{otherwise} \end{cases} . \tag{2}$$

A most general tile assignment for a partition $P \in X$ can be found as follows. We start with a function $f_0 : P \to \Sigma^4$ that assigns to each tile edge a unique glue type, or in other words, a function f_0 so that the mapping $(p, D) \mapsto f_0(p)_D$ is injective. Next, we go through all pairs of adjacent positions in $[m] \times [n]$ (in some order) and require their matching sides to have the same glue type by merging the corresponding glues. This process generates a sequence of functions $f_0, f_1, f_2, \ldots, f_N = f$ and terminates after $N \leq 2mn$ steps.

Lemma 4. *The above algorithm generates a most general tile assignment.*

Proof. By the end, we are left with a function f that satisfies property *A1* by construction. To see why property *A2* is satisfied, we again use the language of partitions.

Any assignment gives rise to a set of equivalence classes (or a partition) on $P \times \mathcal{D}$: Elements that are assigned the same glue type reside in the same equivalence class. The initial assignment f_0 gives each part-direction pair a unique glue type, and thus, corresponds to the initial partition $J = \{\{a\} \mid a \in P \times \mathcal{D}\}$. In the algorithm, any glue merging operation corresponds to the combining of two equivalence classes.

The algorithm goes through a list of pairs $\{\{a_i, b_i\}\}_{i=0}^{N-1}$ of elements from $P \times \mathcal{D}$ that are required to have the same glue type. In this way, the list records

necessary conditions for property *A1* to hold. This is to say that every assignment satisfying *A1* has to correspond to a partition that is coarser than each of the partitions in $\mathcal{L} = \{J[a_i, b_i]\}_{i=0}^{N-1}$, where $J[a, b]$ is the partition obtained from the initial partition by combining parts a and b. Since the set $(P \times \mathcal{D}, \sqsubseteq)$ is a lattice, there exists a unique greatest lower bound $\inf \mathcal{L}$ of the partitions in $\mathcal{L}$. This is exactly the partition that the algorithm calculates in the form of the assignment f. As a greatest lower bound, $\inf \mathcal{L}$ is finer than any partition corresponding to an assignment satisfying *A1*, but this is precisely the requirement for condition *A2*. □

The above analysis also gives the following.

Corollary 5. *For a given partition, MGTAs are unique up to relabeling of the glue types.*

Thus, for each partition P, we take *the MGTA for* P to be some canonical representative from the class of MGTAs for P.

For efficiency purposes, it is worth mentioning that MGTAs can be generated iteratively: A partition $P \in X$ can be obtained by repeatedly combining parts starting from the initial partition I:

$$I = P_1 \sqsupseteq P_2 \sqsupseteq \cdots \sqsupseteq P_N = P \ . \tag{3}$$

As a base case, a MGTA for I can be computed by the above algorithm. A MGTA for each P_{i+1} can be computed from a MGTA for the previous partition P_i by just a small modification: Let a MGTA $f_i : P_i \to \Sigma^4$ be given for P_i and suppose P_{i+1} is obtained from P_i by combining parts $p_1, p_2 \in P_i$. Now, a MGTA f_{i+1} for P_{i+1} can be obtained from f_i by *merging tiles* $f_i(p_1)$ and $f_i(p_2)$, that is, merging the glue types on the four corresponding sides.

We now give the conditions for a partition to be constructible in terms of MGTAs.

Lemma 6. *A partition $P \in X$ is constructible iff the MGTA $f : P \to \Sigma^4$ for P is injective and the tile set $f(P)$ is deterministic in the sense of Proposition 1.*

Proof. "⇒": Let $P \in X$ be constructible and let the MGTA $f : P \to \Sigma^4$ for P be given. Let $\mathscr{T}$ be a deterministic TAS such that $P(\mathscr{T}) = P$. The uniquely produced assembly of $\mathscr{T}$ induces a tile assignment $g : P \to \Sigma^4$ that satisfies property *A1*. Now using property *A2* for the MGTA f we see that any violation of the injectivity of f or any violation of the determinism of the tile set $f(P)$ would imply such violations for g. But since g corresponds to a constructible partition, no violations can occur for g and thus none for f.

"⇐": Let $f : P \to \Sigma^4$ be an injective MGTA with deterministic tile set $f(P)$. Because $f(P)$ is deterministic, we can choose glue types for a seed assembly $\mathcal{S}$ so that the westernmost and southernmost tiles fall into place according to f in the self-assembly process. The TAS $\mathscr{T} = (f(P), \mathcal{S}, s, 2)$, with appropriate glue strengths s, then uniquely produces a terminal assembly that agrees with f on $[m] \times [n]$. This gives $P(\mathscr{T}) \sqsubseteq P$, but since f is injective, $|P| = |f(P)| = |P(\mathscr{T})|$ and so $P(\mathscr{T}) = P$. □

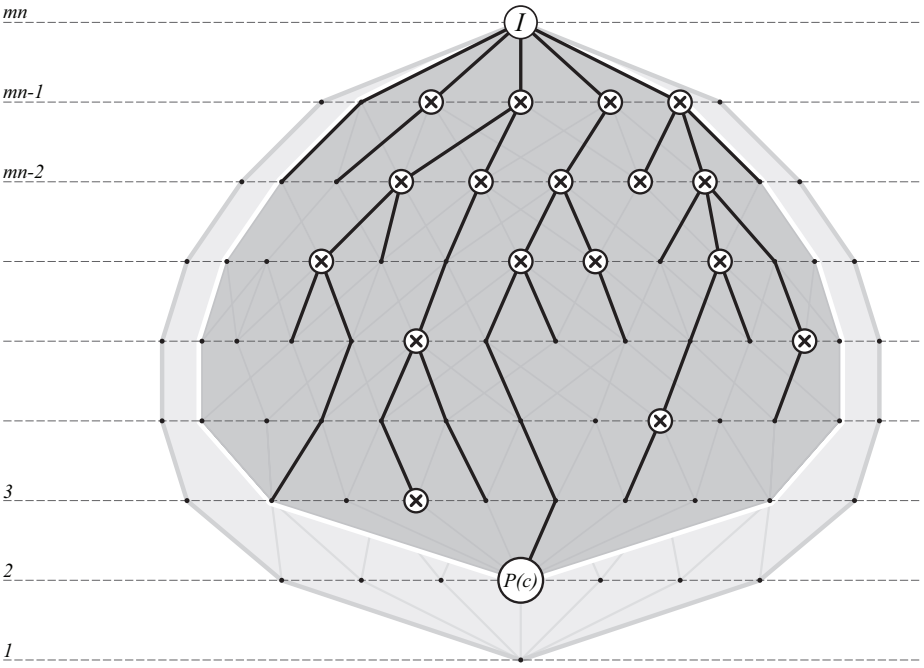

Figure 5: The search tree in the lattice $(X, \sqsubseteq)$. We start with the initial partition I of size $|I| = mn$. The partition $P(c)$ defines the PATS problem instance: We search for constructible partitions (drawn as crosses) in the sublattice (shaded with darker grey) consisting of those partitions that are refinements of $P(c)$. The search tree branches only at the constructible partitions and the tree branches are vertex-disjoint.

4. Complete search for minimal tile sets

We now extend the techniques of [19] to obtain an exhaustive branch-and-bound search method to find minimal solutions to the PATS problem. We call this approach the *partition-search branch-and-bound (PS-BB) algorithm*. The idea of Ma and Lombardi [19] (following experimental work of [21]) is to start with an *initial tile set* that consists of $m \cdot n$ different tiles, one for each of the grid positions in $[m] \times [n]$. Their algorithm then proceeds to merge tile types in order to minimise $|T|$. We formalize this search process as an exhaustive search in the set of all partitions of the set $[m] \times [n]$. In the following, we let a PATS instance be given by a fixed k-coloured pattern $c : [m] \times [n] \to [k]$.

The PS-BB algorithm performs an exhaustive search in the lattice $(X, \sqsubseteq)$ searching for constructible partitions (cf. Figure 5). We start with the initial partition I that is always constructible. In the search, we maintain and incrementally update MGTAs for every partition we visit. First, we describe simple branching rules for the search and later give rules to prune this search tree.

The root of the search tree is taken to be the initial partition I. For each partition $P \in X$ we next define the set $C(P) \subseteq X$ of children of P. Our algorithm always proceeds by combining parts of the partition currently being

visited, so for each $P' \in C(P)$ we will have $P' \sqsubseteq P$. Say we visit a partition $P \in X$. We have two possibilities:

C1. *P is constructible:*

1. If P is not a refinement of the target pattern $P(c)$, that is if $P(c) \not\sqsubseteq P$, we can drop this branch of the search, since no possible descendant $P' \sqsubseteq P$ can be a refinement of $P(c)$ either.
2. In case $P(c) \sqsubseteq P$, we can use the MGTA for P to give a concrete solution to the PATS problem instance defined by the colouring c. To continue the search and to find further improved solutions we consider each pair of parts $\{p_1, p_2\} \subseteq P$ in turn and recursively visit the partition $P[p_1, p_2]$ where the two parts are combined. In fact, by the above analysis, it is sufficient to consider only pairs of the same colour. So, in this case,

$$C(P) = \{P[p_1, p_2] \mid p_1, p_2 \in P,\ p_1 \neq p_2,\ \exists k \in P(c) : p_1, p_2 \subseteq k\}\ . \tag{4}$$

C2. *P is not constructible:* In this case the MGTA f for P gives $f(p_1)_S = f(p_2)_S$ and $f(p_1)_W = f(p_2)_W$ for some parts $p_1 \neq p_2$. We continue the search from partition $P[p_1, p_2]$.

To guarantee that our algorithm finds the optimal solution in the case C2 above, we need the following.

Lemma 7. *Let $P \in X$ be a non-constructible partition, f the MGTA for P and $p_1, p_2 \in P$, $p_1 \neq p_2$, parts such that $f(p_1)_S = f(p_2)_S$ and $f(p_1)_W = f(p_2)_W$. For all constructible $C \sqsubseteq P$ we have $C \sqsubseteq P[p_1, p_2]$.*

Proof. Let P, f, p_1 and p_2 be as in the statement of the lemma. Let $C \sqsubseteq P$ be a constructible partition and $g : C \to \Sigma^4$ the MGTA for C. Since C is coarser than P we can obtain from g a tile assignment $g' : P \to \Sigma^4$ such that $g'(p) = g(q)$, where $q \in C$ is the unique part for which $p \subseteq q$. The assignment g' has property *A1* and so using *A2* for the MGTA f we get that

$$f(p_1)_S = f(p_2)_S \quad \& \quad f(p_1)_W = f(p_2)_W \implies g'(p_1)_S = g'(p_2)_S \quad \& \quad g'(p_1)_W = g'(p_2)_W. \tag{5}$$

Now, since C is constructible, the identities $g(q_1)_S = g(q_2)_S$ and $g(q_1)_W = g(q_2)_W$ can not hold for any two different parts $q_1, q_2 \in C$. Looking at the definition of g', we conclude that $p_1 \subseteq q$ and $p_2 \subseteq q$ for some $q \in C$. This demonstrates $C \sqsubseteq P[p_1, p_2]$. □

4.1. Pruning the search tree

Computational resources should be saved by not visiting any partition twice. To keep the branches in our search tree vertex-disjoint, we maintain a list of

graphs that store restrictions on the choices the search can make. For each partition $P \sqsupseteq P(c)$ we associate a family of undirected graphs $\{G_k^P\}_{k \in P(c)}$, one for each colour class of the pattern $P(c)$. Every part in P is represented by a vertex in the graph corresponding to the colour of the part. More formally, the vertex set $V(G_k^P)$ of the graph G_k^P is taken to be those parts $p \in P$ for which $p \subseteq k$. (So now, $\bigcup_{k \in P(c)} V(G_k^P) = P$.) The edge sets $E(G_k^P)$ are defined by induction on the structure of the search tree. An edge $\{p_1, p_2\} \in E(G_k^P)$ means that the parts p_1 and p_2 are not allowed ever to be combined in the search branch in question. When we start our search with the initial partition I, the edge sets are initially empty, $E(G_k^I) = \emptyset$. At each partition P, the graphs $\{G_k^P\}_{k \in P(c)}$ have been determined by induction and the graphs for those children $P' \in C(P)$ that we visit are defined as follows.

D1. *If P is constructible:* We choose some ordering $\{p_i, q_i\}$, $i = 1, \ldots, N$ of similarly coloured pairs of parts. Define $l_i \in P(c)$, $1 \leq i \leq N$ to be the colour of the pair $\{p_i, q_i\}$, so that $p_i, q_i \subseteq l_i$. Now, we visit a partition $P[p_i, q_i]$ only if $\{p_i, q_i\} \notin E(G_{l_i}^P)$. If we decide to visit a child partition $P' = P[p_j, q_j]$, we define the edge sets $\{E(G_k^{P'})\}_{k \in P(c)}$ as follows:

   1. We start with the graphs $\{G_k^P\}_{k \in P(c)}$ and add the edges $\{p_i, q_i\}$ for all $1 \leq i < j$ to their corresponding graphs. Call the resulting graphs $\{G_k^\star\}_{k \in P(c)}$.
   2. Finally, as we combine the parts p_j and q_j to obtain the partition $P[p_j, q_j]$, we merge the vertices p_j and q_j in the graph $G_{l_j}^\star$ (After merging, the neighbourhood of the new vertex $p_j \cup q_j$ is the union of the neighbourhoods for p_j and q_j in $G_{l_j}^\star$). The graphs $\{G_k^{P'}\}_{k \in P(c)}$ follow as a result.

D2. *If P is not constructible:* Here, the MGTA for P suggests a single child partition $P' = P[p_1, p_2]$ for some $p_1, p_2 \subseteq l \in P(c)$. If $\{p_1, p_2\} \in E(G_l^P)$, we terminate this branch of the search. Otherwise, we define the graphs $\{G_k^{P'}\}_{k \in P(c)}$ to be the graphs $\{G_k^P\}_{k \in P(c)}$, except that in $G_l^{P'}$ the vertices p_1 and p_2 have to be merged.

One can see that the outcome of this pruning process is a search tree that has vertex-disjoint branches and one in which every possible constructible partition is still guaranteed to be found. Figure 5 presents a sketch of the search tree. Note that we are not usually interested in finding every constructible partition $P \in X$, but only in finding a minimal one (in terms of $|P|$). Next, we give an efficient method to lower-bound the partition sizes of a given search branch.

4.2. The bounding function

Given a root $P \in X$ of some subtree of the search tree, we ask: What is the smallest partition that can be found from this subtree? The vertices in the subtree rooted at P comprise those partitions $P' \sqsubseteq P$ that can be obtained from P by merging pairs of parts that are not forbidden by the graphs $\{G_k^P\}_{k \in P(c)}$.

This merging process halts precisely when all the graphs $\{G_k^{P'}\}_{k\in P(c)}$ have been reduced into cliques. As is well known, the size of the smallest clique that a graph G can be turned into by merging non-adjacent vertices is given by the *chromatic number*[6] $\chi(G)$ of the graph G. This immediately gives the following.

Proposition 8. *For every $P' \sqsubseteq P$ in the subtree rooted at P and constrained by $\{G_k^P\}_{k\in P(c)}$, we have*

$$\sum_{k\in P(c)} \chi(G_k^P) \;\leq\; |P'| \;. \tag{6}$$

Determining the chromatic number of an arbitrary graph is an NP-hard problem. Fortunately, we can restrict our graphs to be of a special form: graphs that consist only of a clique and some isolated vertices. For these graphs, the chromatic numbers are given by the sizes of the cliques.

To see how to maintain graphs in this form, consider as a base case the initial partition I. Here, $E(G_k^I) = \emptyset$ for all $k \in P(c)$, so G_k^I is of our special form—it has a clique of size 1. For a general partition P, we go through the branching rules D1-D2.

D1: *P is constructible:* Since we are allowed to choose an arbitrary ordering $\{p_i, q_i\}$, $i = 1, \ldots, N$ for the children $P[p_i, q_i]$, we design an ordering that preserves the special form of the graphs. For a graph G of our special form, let $K(G) \subseteq V(G)$ consist of those vertices that are part of the clique in G. In the algorithm, we first set $H_k = G_k^P$ for all $k \in P(c)$ and repeat the following process until every graph H_k is a complete clique.

1. Pick some colour $k \in P(c)$ and an isolated vertex $v \in V(H_k) \setminus K(H_k)$.
2. Process the pairs $\{v, u\}$ for all $u \in K(H_k)$ in some order. By the end, update H_k to include all the edges $\{v, u\}$ that were just processed (the size of the clique in H_k increases by one).

A moment's inspection reveals that when the graphs G_k^P are of our special form, so are all of the derived graphs passed on to the children of P.

D2: *P is not constructible:* If the algorithm decides to continue the search from a partition $P' = P[p_1, p_2]$, for some $p_1, p_2 \subseteq l \in P(c)$, we have $\{p_1, p_2\} \notin E(G_l^P)$. This means that either $p_1, p_2 \in V(G_l^P) \setminus K(G_l^P)$, in which case we are merging two isolated vertices, or one of p_1 or p_2 is part of the clique $K(G_l^P)$, in which case we merge an isolated vertex to the clique. In both cases, we maintain the special form in the graphs $\{G_k^{P'}\}_{k\in P(c)}$.

[6]The chromatic number of a graph G is the smallest number of colours $\chi(G)$ needed to colour the vertices of G so that no two adjacent vertices share the same colour.

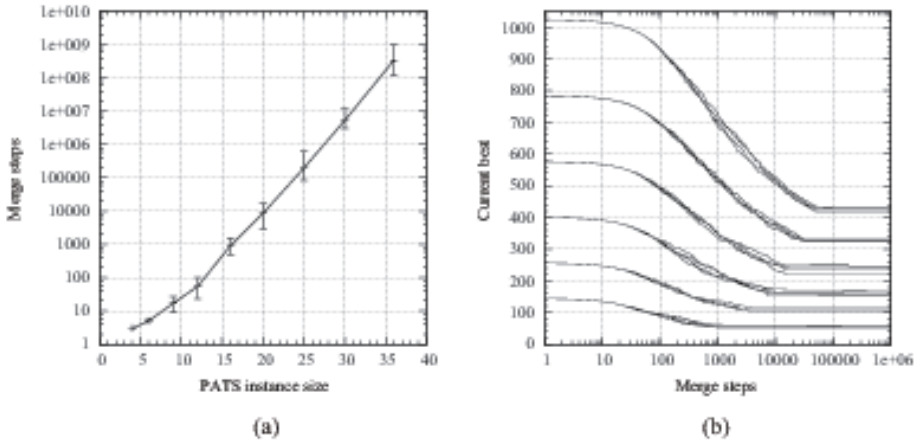

Figure 6: (a) Running time of the PS-BB algorithm (as measured by the number of merge operations) to solve random 2-coloured near-square-shaped instances of the PATS problem. (b) Evolution of the tile set size of the "current best solution" for several large random 2-coloured instances of the PATS problem.

4.3. Traversing the search tree

When running a branch-and-bound algorithm we maintain a "current best solution" discovered so far as a global variable. This solution gives an upper bound for the minimal value of the tile set size and can be used to prune such search branches that are guaranteed (by the bounding function) to only yield solutions worse than the current best. There are two general strategies to traverse a branch-and-bound search tree: *Depth-First Search* and *Best-First Search* [1]. Our description of the search tree for the lattice X is general enough to allow either of these strategies to be used in the actual implementation of the algorithm. In the following Results section we give performance data on a DFS implementation of the PS-BB algorithm.

4.4. Results

The running time of the PS-BB algorithm is proportional—up to a polynomial factor—to the number of partitions the algorithm visits. Hence, we measure the running time in terms of the number of merge operations performed in the search. Figure 6(a) presents the running time of the algorithm to find a minimal solution for random 2-coloured instances of the PATS problem. The algorithm was executed for instance sizes $2 \times 2, 2 \times 3, 3 \times 3, \cdots, 5 \times 6$ and 6×6; the 20th and 80th percentiles are shown alongside the median of 21 separate runs for each instance size. For the limiting case 6×6, the algorithm spent on the order of two hours of (median) computing time on a 2,61 GHz AMD processor.

Even though branch-and-bound search is an exact method, it can be used to find approximate solutions by running it for a suitable length of time. Figure 6(b) illustrates how the best solution found up to a point develops as increasingly

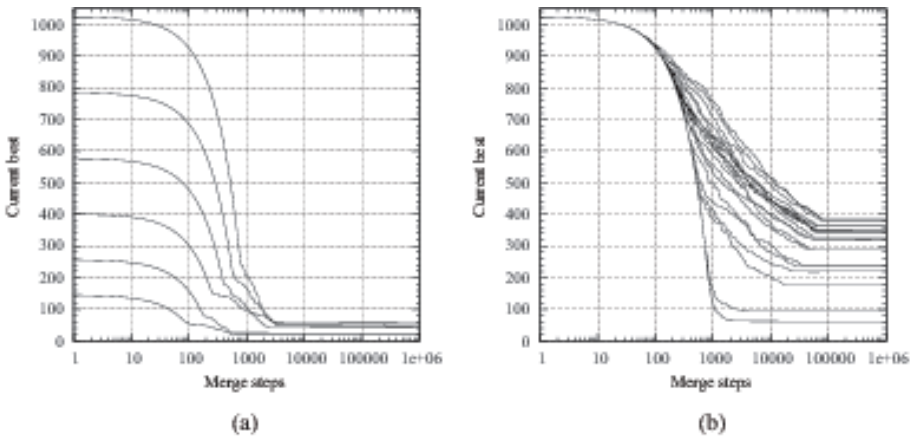

Figure 7: Evolution of the "current best solution" of the PS-BB algorithm for (a) the Sierpinski pattern and for (b) the binary counter pattern. Randomisation in the DFS has a clear effect on the performance of the algorithm in the case of the binary counter pattern.

many steps of the algorithm are run. The figure provides data on random 2-coloured instances of sizes from 12×12 up to 32×32. Because we begin our search from the initial partition, the best solution at the first step is precisely equal to the instance size. For each size, several different patterns were used. The algorithm was cut off after 10^6 steps. By this time, an approximate reduction of 58% in the size of the tile set was achieved (cf. a reduction of 43.5% in [19]).

Next, we consider two well known examples of structured patterns: the discrete Sierpinski triangle (part of which was shown in Figure 2) and the binary counter (see Figures 8(a) and 8(b) for 32×32 instances of both patterns). A tile set of size 4 is optimal for both of these patterns. First, for the Sierpinski pattern, we get a tile reduction of well over 90% (cf. 45% in [19]) in Figure 7(a). We used the same cutoff threshold and instance sizes as in Figure 6(b).

Our description of the PS-BB algorithm leaves some room for randomisation in deciding which search branch the DFS search is to explore next. This randomisation does not seem to affect the search dramatically when considering the Sierpinski pattern—the separate single runs in Figure 7(a) are representative of an average randomised run. By contrast, for the binary counter pattern, randomised runs for a single instance size do make a difference. Figure 7(b) depicts several separate runs for instance size 32×32. Here, each run brings about a reduction in solution size that oscillates between a reduction achieved on a random 2-coloured instance (6(b)) and a reduction achieved on the Sierpinski instance (7(a)). This suggests that, as is characteristic of DFS traversal, restarting the algorithm with different random seeds may help with large instances that have small optimal solutions. We explore this opportunity for efficiency improvement further in connection to the algorithm PS-H presented in the next Section.

5. Heuristically guided search for small tile sets

5.1. The PS-H algorithm scheme

The PS-BB algorithm utilises effective pruning methods to reduce the search space. Even though it offers significant reduction in the size of tile sets compared to earlier approaches, it is in most cases still too slow for patterns of practical size. Often it is not important to find a provably minimal solution, but to find a reasonably small solution in reasonable amount of time. To address this objective, we present in the following a modification of the basic PS-BB algorithm with a number of search-guiding heuristics. We call this approach the *partition-search with heuristics (PS-H) algorithm scheme*.

Whereas the pruning heuristics of the PS-BB algorithm try to reduce the size of the search space in a "balanced" way, the PS-H algorithm attempts to "greedily" optimise the order in which the coarsenings of a partition are explored, in the hope of being directly lead to close-to-optimal solutions. Such opportunism may be expected to pay off in case the success probability of the greedy exploration is sufficiently high, and the process is restarted sufficiently often, or equivalently, several runs are explored in parallel.

The basic heuristic idea is to try to minimise the effect that a merge operation has on other partition classes than those which are combined. This can be achieved by preferring to merge classes already having as many common glues as possible. In this way one hopes to extend the number of steps the search takes before it runs into a conflict. For example, when merging classes p_1 and p_2 such that $f(p_1)_N = f(p_2)_N$ and $f(p_1)_E = f(p_2)_E$, the glues on the W and S edges of all other classes are unaffected. This way, the search avoids proceeding to a partition which is not constructible after the merge operation is completed. Secondarily, we prefer merging classes which already cover a large number of sites in $[m] \times [n]$. That is, one tries to grow a small number of large classes instead of growing all the classes at an equal rate.

We define the concept of the *number of common glues* formally as follows.

Definition 3. *Given a partition P and a MGTA f for P, the* number of common glues *between classes $p, q \in P$ is defined by the function $G : P \times P \to \{0, 1, 2, 3, 4\}$,*

$$G(p, q) = \sum_{D \in \mathcal{D}} g(f(p)_D, f(q)_D),$$

where $g(\sigma_1, \sigma_2) = 1$ if $\sigma_1 = \sigma_2$ and 0 otherwise, for all $\sigma_1, \sigma_2 \in \Sigma$.

Except for the bounding function, the PS-BB algorithm allows an arbitrary ordering $\{p_i, q_i\}, i = 1, \ldots, N$, for the children (coarsenings) $P[p_i, q_i]$ of a constructible partition P. In the PS-H algorithm, we choose the ordering using the following heuristic. First form the set

$$H := \{\{p, q\} \mid p, q \in P,\ p \neq q,\ \exists r \in P(c) :\ p, q \subseteq r\}$$

of class pairs of same colour, and then repeat the following process until H is empty.

H1. Set $K := H$.

H2. Maximise the number of common glues:

$$K := \{\{p, q\} \in K \mid G(p, q) \geq G(u, v) \text{ for all } \{u, v\} \in K\}.$$

H3. Maximise the size of the larger class:

$$K := \{\{p, q\} \in K \mid \max\{|p|, |q|\} \geq \max\{|u|, |v|\} \text{ for all } \{u, v\} \in K\}.$$

H4. Maximise the size of the smaller class:

$$K := \{\{p, q\} \in K \mid \min\{|p|, |q|\} \geq \min\{|u|, |v|\} \text{ for all } \{u, v\} \in K\}.$$

H5. Pick some pair $\{p, q\} \in K$ at random and visit the partition $P[p, q]$.

H6. Remove $\{p, q\}$ from H:

$$H := H \setminus \{\{p, q\}\}.$$

The PS-H algorithm also omits the pruning process utilised by the PS-BB algorithm. That way, it aims to get to the small solutions quickly by reducing the computational resources used in a single merge operation.

Since step H5 of the heuristic above leaves room for randomisation, the PS-H algorithm performs differently with different random seeds. While some of the randomised runs may lead to small solutions quickly, others may get sidetracked into worthless expanses of the solution space. We make the best of this situation by running several executions of the algorithm in paraller, or equivalently, restarting the search several times with a different random seed. The notation PS-H$_n$ denotes the heuristic partition search algorithm with n parallel search threads. The solution found by the PS-H$_n$ algorithm is the smallest solution found by any of the n paraller threads.

5.2. Results

In this section, we present results on the performance of the PS-H$_n$ algorithm for $n = 1, 2, 4, 8, 16,$ and 32 and compare it to the previous PS-BB algorithm. We consider several different finite 2-coloured input patterns, two of which were analysed also previously using the PS-BB algorithm: the discrete Sierpinski triangles of sizes 32×32 (Figure 8(a)) and 64×64, and the binary counter of size 32×32 (Figure 8(b)). Furthermore, we introduce a 2-coloured "tree" pattern of size 23×23 (Figure 8(c)) as well as a 15-coloured pattern of size 20×10 based on a CMOS full adder design (Figure 8(d)). For an explanation of the notation used in Figure 8(d), see the attached Supplementary Information detailing on the tile-based high-level design scheme for nano-electric circuits introduced in [2]. While the Sierpinski triangle and binary counter patterns are known to have minimal solutions of four tiles, the minimal solutions for the tree pattern and the full adder pattern are unknown.

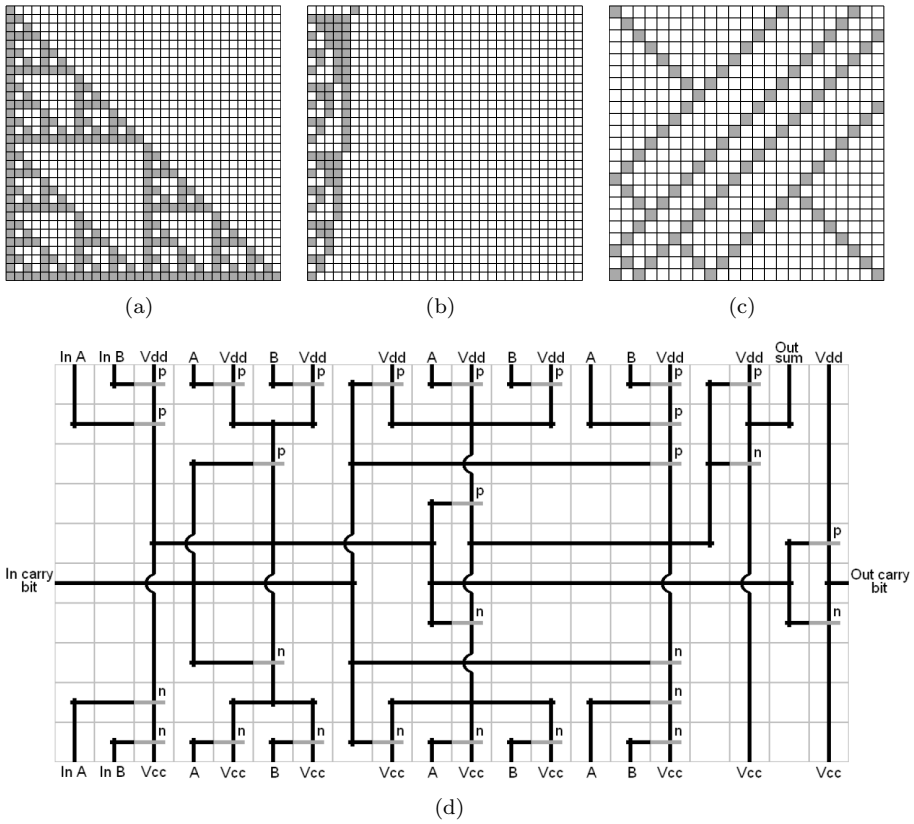

Figure 8: (a) The 32×32 Sierpinski triangle pattern. (b) The 32×32 binary counter pattern. (c) The 23×23 "tree" pattern. (d) A CMOS full adder design that induces a 15-colour 20×10 pattern.

Figure 9 presents the evolution of the "current best solution" as a function of time for the (a) 32×32 and (c) 64×64 Sierpinski patterns. To allow fair comparison, Figures 9(b) and 9(d) present the same data with respect to the total processing time taken by all the parallely running executions. The experiments were repeated 21 times and the median of the results is depicted. In 37% of all the runs conducted, the PS-H algorithm is able to find the optimal 4-tile solution for the 32×32 Sierpinski pattern in less than 30 seconds. The similar percentage for the 64×64 Sierpinski pattern is 34% in one hour. Remarkably, the algorithm performs only from 1030 to 1035 and from 4102 to 4107 merge steps before arriving at the optimal solution for the 32×32 and 64×64 patterns, respectively. In other words, the search rarely needs to backtrack. In contrast, the smallest solutions found by the PS-BB algorithm have 42 tiles, reached after $1.4 \cdot 10^6$ merge steps, and 95 tiles, reached after $5.9 \cdot 10^6$ merge steps.

In Figure 10 we present the corresponding results for the 32×32 binary counter and 23×23 tree patterns. The size of the smallest solutions found by

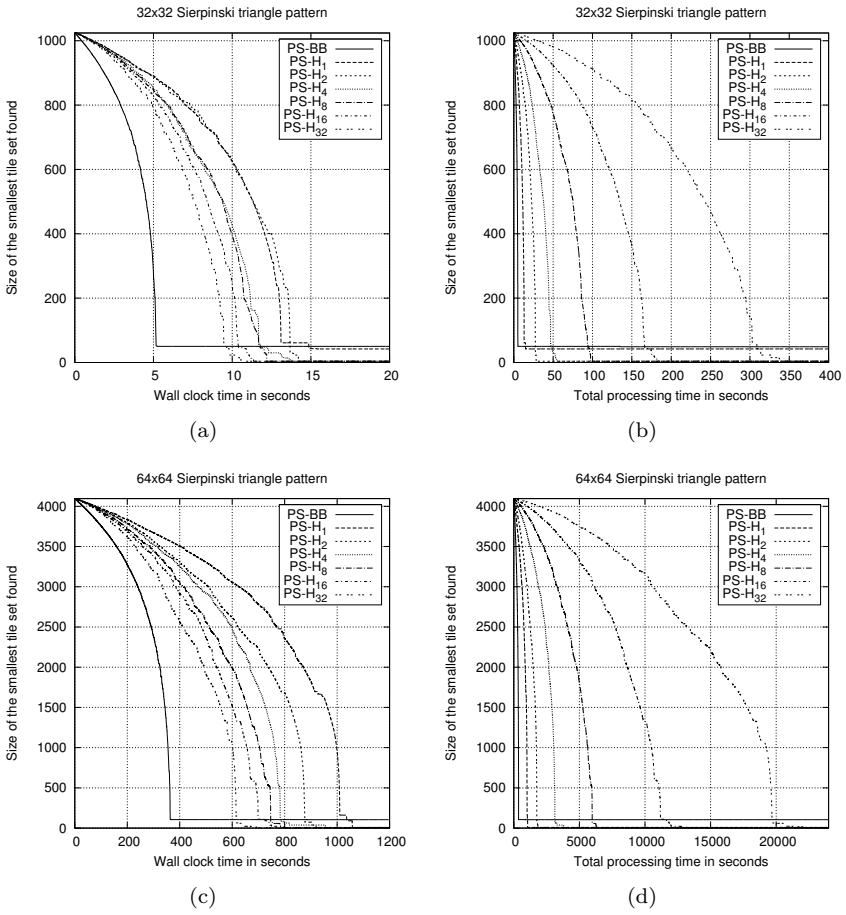

Figure 9: Evolution of the smallest tile set found for the 32×32 and 64×64 Sierpinski triangle patterns as a function of time. The time axis measures (a), (c) wall clock time and (b), (d) wall clock time multiplied by the number of parallel executions.

the PS-H_{32} algorithm were 20 (cf. 307 by PS-BB) and 25 (cf. 192 by PS-BB) tiles, respectively. In the case of the tree pattern, the parallelisation brings significant advantage over a single run. Finally, Figures 11(a)-11(b) show the results for the 20×10 15-colour CMOS full adder pattern. In this case, the improvement over the previous PS-BB algorithm is less clear. The PS-H_{32} algorithm is able to find a solution of 58 tiles, whereas the PS-BB algorithm gives a solution of 69 tiles.

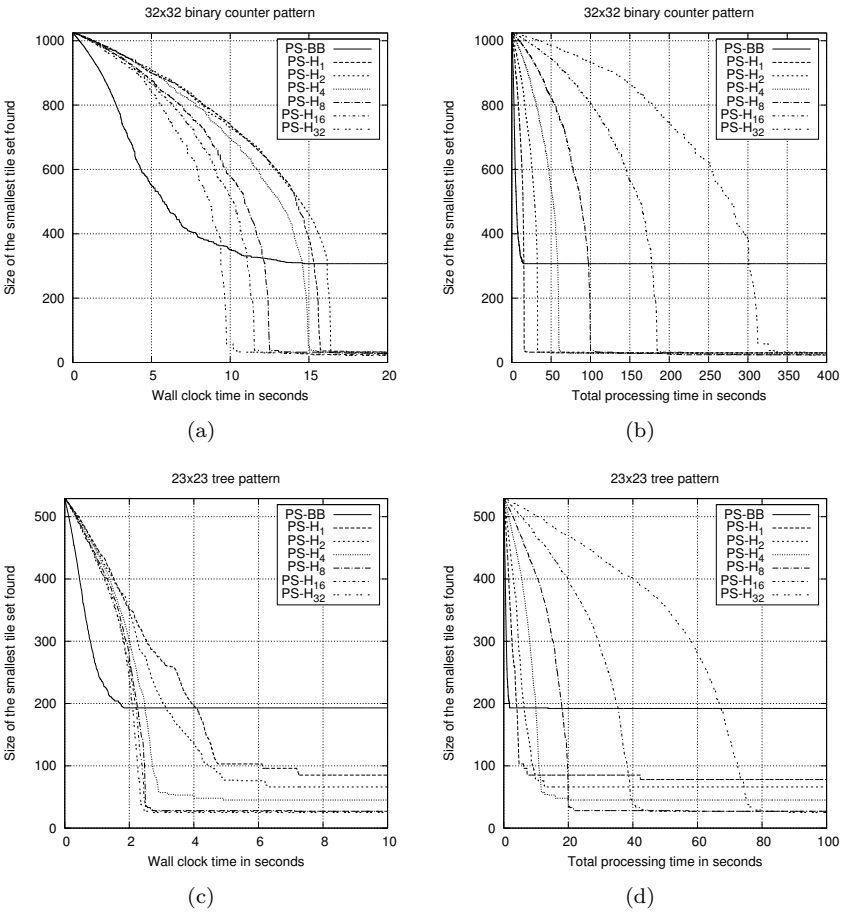

Figure 10: Evolution of the smallest tile set found for the 32×32 binary counter and 23×23 tree patterns as a function of time. The time axis measures (a), (c) wall clock time and (b), (d) wall clock time multiplied by the number of parallel executions.

6. Answer set programming for minimal tile sets

6.1. ASP model for PATS

Answer Set Programming (ASP) [13] is a declarative logic programming paradigm for solving difficult combinatorial search problems. In ASP, a problem is described as a logic program, and an answer set solver is then used to compute stable models (answer sets) for the logic program.

The ASP paradigm can be applied also to the PATS problem. In the following we give a brief description on how to transform the PATS problem to an ASP program using the LPARSE [29] language. First, we define a constant for each position of the grid $[m] \times [n]$, each colour, each available tile type and each available glue type. After that, a number of choice rules are introduced

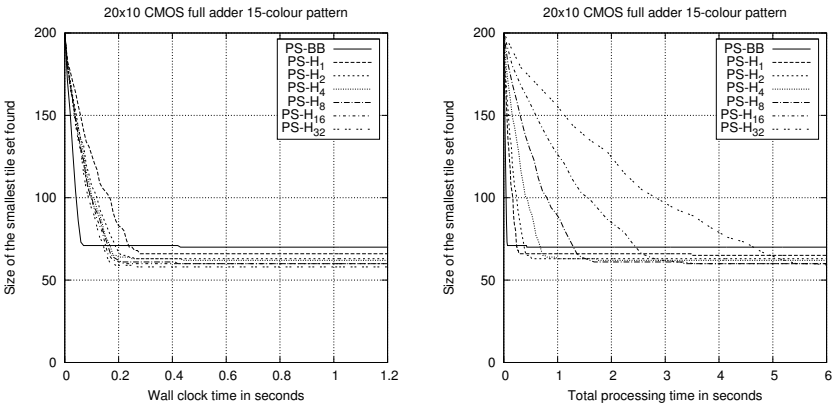

(a) (b)

Figure 11: (a)-(b) Evolution of the smallest tile set found for the 20×10 full adder pattern as a function of time. The time axis measures (a) wall clock time and (b) wall clock time multiplied by the number of parallel executions.

to associate a tile type with each position of the grid, a glue type with each of the four sides of the tile types and a colour with each of the tile types. Choice rules are also used to make the glues of every pair of adjacent tiles to match and to make the tile system deterministic, i.e. to ensure that every tile type has a unique pair of glues on its W and A edges.

We finally compile the target pattern to a set of rules that associate every position of the grid with a colour. This description of the pattern is combined with the above-described program and given to an answer set solver, which then outputs a tile type for each position of the grid, given that such a solution exists. The program is run several times using an increasing number of available tile and glue types, until a solution is found.

6.2. Results

We used the answer set solver SMODELS [29] to run our experiments. We consider two patterns having a minimal solution of four tiles, the Sierpinski triangle and the binary counter. The program was executed for pattern sizes $1 \times 1, 2 \times 2, 3 \times 3, \ldots, 100 \times 100$. The running time of the program is presented in Figure 12(a) for the Sierpinski triangle and in Figure 12(b) for the binary counter. SMODELS was able to find the minimal solution for the 100×100 Sierpinski triangle in little over 5 hours and for the 100×100 binary counter in less than two hours. The running time grows rather consistently with the pattern size, but interestingly, there are a few notable exceptions. The running times for the 49×49 and 55×55 Sierpinski patterns, not shown in the figure, are close to 40 hours and close to 10 hours, respectively. That is clearly out of line with other proximate pattern sizes. For the binary counter patterns of size 29×29, 35×35 and 60×60 SMODELS was not able to find a solution in

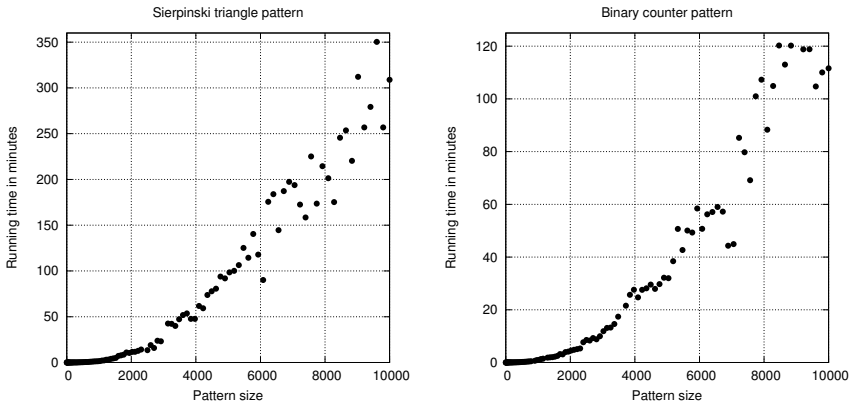

Figure 12: (a),(b) Running time of SMODELS for the minimal solutions of the Sierpinski triangle and binary counter patterns as a function of pattern size.

less than 48 hours. Thus, the running times for those instances are also missing from the figure.

Based on the above results, the ASP approach performs well when considering patterns with a small minimal solution. However, the running time seems to increase dramatically with patterns having a larger minimal solution.

7. Reliability of tile sets

7.1. The Kinetic Tile Assembly Model

In the following, we use the kinetic Tile Assembly Model (kTAM) in order to asses the reliabilities of various tile sets generated by the PS-BB and PS-H algorithms. The kTAM has been introduced by Winfree [30] as a kinetic counterpart of the aTAM. Several variants of the kTAM exist, see e.g. [6, 27]. However, the main elements are similar.

The kTAM simulates two types of reactions, each involving an assembly, i.e. a crystal structure consisting of several merged tiles, and a tile: *association* of tiles to the assembly (forward reaction) and *dissociation* (reverse reaction), see e.g. Figure 13.[7] In the first type of reaction, any tile can attach to the assembly at any position (up to the assumption that tile alignment is preserved), even if only a weak bond is formed; the rate of this reaction r_f is proportional to the concentration of free tiles in the solution. In the second type of reaction, any tile can detach from the assembly with rate $r_{r,b}$, $b \in \{0, \ldots, 4\}$, which is

[7]Note that interactions between two tiles, such as forming a new assembly, as well as interactions between two assemblies, are not taken into consideration in the initial model [30]. However, they are studied in some of the later developed variants of the kTAM, see e.g. [27].

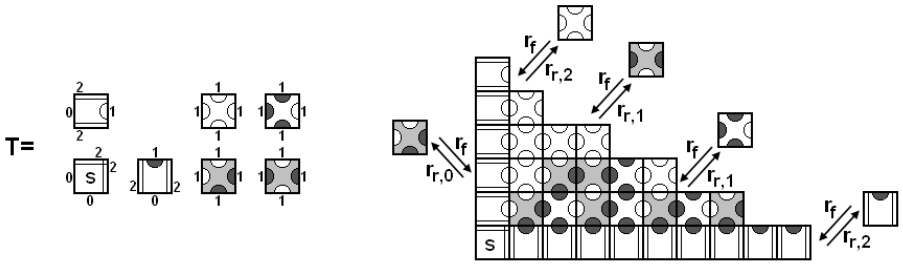

Figure 13: Possible association and/or dissociation reactions in the Kinetic Tile Assembly Model. The rate of all association reactions is identical; the rates of the dissociation reactions depend on the total strength of the bonds connecting a tile to the assembly.

exponentially correlated with the total strength of the bonds between the tile and the assembly. Thus, tiles which are connected to the assembly by fewer or weaker bonds, i.e. incorrect "sticky end" matches, are more prone to dissociation than those which are strongly connected by several bonds (well paired sticky end sequences).

In the following, we follow the notation of [30]. For any tile type t, the rate constant r_f of the association (forward reaction) of t to an existing assembly is given by

$$r_f = k_f[t], \ (\text{insec}^{-1})$$

where $[t]$ is the concentration in solution of free tiles of type t and k_f is a temperature dependent parameter. In the case of DNA double-crossover (DX) tiles, this parameter is given by the formula

$$k_f = A_f e^{-E_f/RT},$$

where $A_f = 5 \cdot 10^8$ /M/sec, $E_f = 4000$ cal/mol, $R = 2$ cal/mol/K, and T is the temperature (in K).

In the case of dissociation (reverse reaction), for a tile which is connected to the assembly by a total bond strength b, the rate constant $r_{r,b}$ is given by the formula

$$r_{r,b} = k_f e^{\Delta G^o_b/RT},$$

where $\Delta G^o_b/RT$ is the standard free energy needed in order to break the b bonds. In the case of DX tiles, as the glues of the tiles are implemented using 5-base long single-stranded DNA molecules, ΔG^o_b can be estimated using the nearest-neighbour model [17] to

$$\Delta G^o_b = e^{5b\left(11 - \frac{4000 \text{ K}}{T}\right)+3} \text{ cal/mol}.$$

Moreover, b can range with integer values from 0 to 4, corresponding to the cases when the tile is totally erroneously placed in the assembly (no bond connects it to the crystal) and when the tile is fully integrated into the assembly (all its four sticky ends are correctly matched), respectively.

In order to easily represent and scale the system, the free parameters involved in the formulas of the rate constants r_f and $r_{r,b}$ are re-distributed into just two dimensionless parameters, G_{mc} and G_{se}, where the first is dependent on the initial tile concentration, while the second is dependent on the assembly temperature:

$$r_f = \hat{k}_f e^{-G_{mc}}, \qquad r_{r,b} = \hat{k}_f e^{-bG_{se}},$$

where, in the case of DX tiles, $\hat{k}_f = e^3 k_f$ is adjusted in order to take into consideration possible entropic factors, such as orientation or location of tiles. The previous parameter re-distribution is made possible as a result of the assumption made in the initial kTAM [30] that all tile types are provided into the solution in similar concentrations, and that the consumption in time of the free monomers is negligible compared to the initial concentration.

7.2. Computing the Reliability of a Tile Set

By choosing appropriate physical conditions, the probability of errors in the assembly process can be made arbitrarily low, at the cost of reducing the assembly rate [30]. However, we would like to be able to compare the error probability of different tile sets producing the same finite pattern, under the same physical conditions. Given the amount of time the assembly process is allowed to take, we define the *reliability of a tile set* to be the probability that the assembly process of the tile system in question completes without any incorrect tiles being present in the terminal configuration. In the following, we present a method for computing the reliability of a tile set, based on Winfree's analysis of the kTAM [30], and the notion of *kinetic trapping* introduced within.

We call the W and S edges of a tile its *input edges*. First, we derive the probability of the correct tile being frozen at a particular site under the condition that the site already has correct tiles on its input edges. Let $M^1_{i,j}$ and $M^2_{i,j}$ be the number of tile types having one mismatching and two mismatching input glues, respectively, between them and the correct tile type for site $(i, j) \in [m] \times [n]$. Now, for a deterministic tile set T, the total number of tiles is $|T| = 1 + M^1_{i,j} + M^2_{i,j}$ for any $(i, j) \in [m] \times [n]$. Given that a site has the correct tiles on its input edges, a tile is correct for that site if and only if it has two matches on its input edges.

In what follows, we assume that correct tiles are attached at sites $(i - 1, j)$ and $(i, j - 1)$. The model for kinetic trapping [30] gives four distinct cases in the situation preceding the site (i, j) being frozen by further growth. To each of these cases we can associate an "off-rate" for the system to exit its current state: (E) An empty site, with "off-rate" $|T|r_f$. (C) The correct tile, with off-rate $r_{r,2}$. (A) A tile with one match, with off-rate $r_{r,1}$. (I) A tile with no matches, with off-rate $r_{r,0}$. Additionally, we have two sink states FC and FI, which represent frozen correct and frozen incorrect tiles, respectively. The rate of a site being frozen is equal to the rate of growth $r^* = r_f - r_{r,2}$. Figure 14 describes the dynamics of the system. Let $p_S(t)$ denote the probability of the site being in state S after t seconds for all $S \in \{\mathrm{E}, \mathrm{C}, \mathrm{A}, \mathrm{I}, \mathrm{FC}, \mathrm{FI}\}$. To compute the frozen

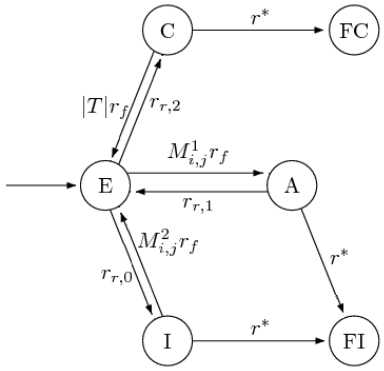

Figure 14: The dynamics of the kinetic trapping model.

distribution, we write the rate equations for the model of kinetic trapping from Figure 14 as follows[8]:

$$M\mathbf{p}(t) := \begin{bmatrix} -|T|r_f & r_{r,2} & r_{r,1} & r_{r,0} & 0 & 0 \\ r_f & -r_{r,2}-r^* & 0 & 0 & 0 & 0 \\ M^1_{i,j}r_f & 0 & -r_{r,1}-r^* & 0 & 0 & 0 \\ M^2_{i,j}r_f & 0 & 0 & -r_{r,0}-r^* & 0 & 0 \\ 0 & r^* & 0 & 0 & 0 & 0 \\ 0 & 0 & r^* & r^* & 0 & 0 \end{bmatrix} \begin{bmatrix} p_{\mathrm{E}}(t) \\ p_{\mathrm{C}}(t) \\ p_{\mathrm{A}}(t) \\ p_{\mathrm{I}}(t) \\ p_{\mathrm{FC}}(t) \\ p_{\mathrm{FI}}(t) \end{bmatrix} = \dot{\mathbf{p}}(t),$$

where $\mathbf{p}(0) = [1 \quad 0 \quad 0 \quad 0 \quad 0 \quad 0]^T$.

To compute the steady-state probability of the site being frozen with the correct tile, i.e., $p_{\mathrm{FC}}(\infty)$, we make use of the steady state of the related flow problem [30][9]:

$$M\mathbf{p}(\infty) = [1 \quad 0 \quad 0 \quad 0 \quad p_{\mathrm{FC}}(\infty) \quad p_{\mathrm{FI}}(\infty)]^T = \dot{\mathbf{p}}(\infty),$$

which gives us a system of linear equations. This system has a single solution, namely

$$p_{\mathrm{FC}}(\infty) = \frac{\frac{1}{r^*+r_{r,2}}}{\frac{1}{r^*+r_{r,2}} + \frac{M^1_{i,j}}{r^*+r_{r,1}} + \frac{M^2_{i,j}}{r^*+r_{r,0}}} = \Pr(C_{i,j} \mid C_{i-1,j} \cap C_{i,j-1}),$$

where $C_{i,j}$ denotes the event of the correct tile being frozen at site (i, j).

The assembly process can be thought of as a sequence of tile addition steps $(a_1, a_2, \ldots, a_N)$ where $a_k = (i_k, j_k)$, $k = 1, 2, \ldots, N$, denotes a tile being frozen at site (i_k, j_k). Due to the fact that the assembly process of the tile systems

[8]The notation $\dot{\mathbf{p}}(x)$ is used to denote the derivative of $\mathbf{p}$ with respect to time.

[9]By the definition of the kinetic trapping model [30], it is assumed that a unit amount of tiles are supplied into state E of the system at any time point.

considered here proceeds uniformly from south-west to north-east, we have that $\{(i_k - 1, j_k), (i_k, j_k - 1)\} \subseteq \{a_1, a_2, \ldots, a_{k-1}\}$ for all $a_k = (i_k, j_k)$. We assume that tiles elsewhere in the configuration do not affect the probability. Now we can compute the probability of a finite-size pattern of size N assembling without any errors, i.e. the reliability of that pattern:

$$\begin{aligned}\Pr(\text{correct pattern}) &= \Pr(C_{a_1} \cap C_{a_2} \cap \cdots \cap C_{a_N}) \\ &= \Pr(C_{a_1})\Pr(C_{a_2} \mid C_{a_1}) \cdots \Pr(C_{a_N} \mid C_{a_1} \cap C_{a_2} \cap \cdots \cap C_{a_{N-1}}) \\ &= \prod_{i,j} \Pr(C_{i,j} \mid C_{i-1,j} \cap C_{i,j-1}).\end{aligned}$$

We have computed the probability in terms of G_{mc} and G_{se}. Given the desired assembly rate, we want to minimise the error probability by choosing values for G_{mc} and G_{se} appropriately. If the assembly process is allowed to take t seconds, the needed assembly rate for an $m \times n$ pattern is approximately $r^* = \frac{\sqrt{m^2+n^2}}{t}$.

$$\Pr(C_{i,j} \mid C_{i-1,j} \cap C_{i,j-1}) = \frac{\frac{1}{r^*+r_{r,2}}}{\frac{1}{r^*+r_{r,2}} + \frac{M^1_{i,j}}{r^*+r_{r,1}} + \frac{M^2_{i,j}}{r^*+r_{r,0}}} \approx \frac{1}{1 + M^1_{i,j}\frac{r^*+r_{r,2}}{r^*+r_{r,1}}}.$$

For small error probability and $2G_{se} > G_{mc} > G_{se}$,

$$\Pr(\neg C_{i,j} \mid C_{i-1,j} \cap C_{i,j-1}) \approx M^1_{i,j}\frac{r^* + r_{r,2}}{r^* + r_{r,1}} \approx M^1_{i,j}e^{-(G_{mc}-G_{se})} =: M^1_{i,j}e^{-\triangle G}.$$

From

$$r^* = r_f - r_{r,2} = \hat{k}_f(e^{-G_{mc}} - e^{-2G_{se}})$$

we can derive

$$G_{se} = -\frac{1}{2}\log(e^{-G_{mc}} - \frac{r^*}{\hat{k}_f}).$$

Now we can write $\triangle G$ as a function of G_{mc}:

$$\triangle G(G_{mc}) = G_{mc} - G_{se} = G_{mc} + \frac{1}{2}\log(e^{-G_{mc}} - \frac{r^*}{\hat{k}_f}).$$

We find the maximum of $\triangle G$, and thus the minimal error probability, by differentation:

$$G_{mc} = -\log(2\frac{r^*}{\hat{k}_f}).$$

Thus, if the assembly time is t seconds, the maximal reliability is achieved at

$$G_{mc} = -\log(2\frac{\sqrt{m^2+n^2}}{t\hat{k}_f}), \qquad G_{se} = -\frac{1}{2}\log(\frac{\sqrt{m^2+n^2}}{t\hat{k}_f}).$$

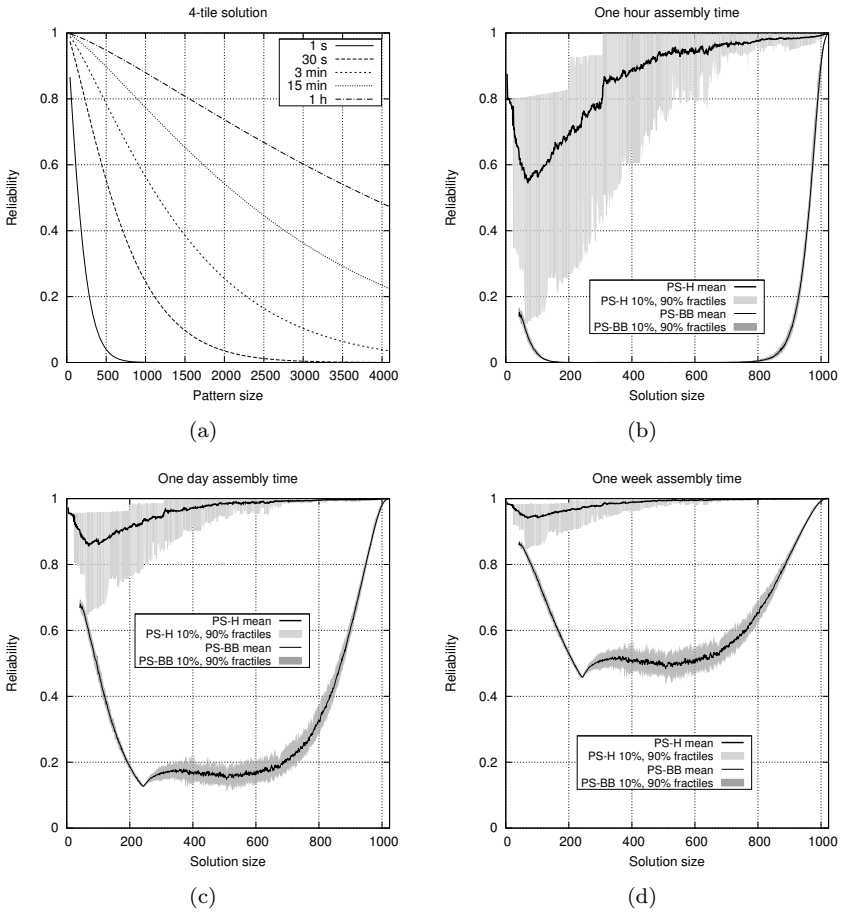

Figure 15: (a) The reliability of the minimal tile set as a function of pattern size for the Sierpinski triangle pattern, using several different assembly times. (b)-(d) The reliability of solutions for the 32×32 Sierpinski triangle pattern found by the PS-H and PS-BB algorithms, allowing assembly time of one hour, one day and one week.

7.3. Results

In this section, we present results on computing the reliability of tile sets using the method presented in Section 7. We assume that the assembly process takes place in room temperature (298 K). As a result, we use the value $k_f = A_f e^{-E_f/RT} \approx 6 \cdot 10^5$ /M/sec for the forward reaction rate.

Figure 15(a) shows the reliability of the 4-tile solution to the Sierpinski triangle pattern as a function of pattern size, using five distinct assembly times. As is to be expected, the longer the assembly time, the better the reliability.

We also applied the method for computing the reliability to tile sets found by the partition search algorithms. Our results show that the heuristics used in the PS-H algorithm improve not only the size of the tile sets found, but also

the reliability of those tile sets. This can be easily understood by considering the following: the reliability of a tile set is largely determined by the number of tile types that have the same glue as some other tile type on either one of their input edges. Since the PS-H algorithm prefers merging class pairs with common glues, it reduces the number of such tile types effectively.

Figures 15(b)–15(d) present the reliability of tile sets found by the PS-H and PS-BB algorithms for the 32×32 Sierpinski triangle pattern, with assembly times of one hour, one day (24 hours) and one week. The runs were repeated 100 times; the mean reliability of each tile set size as well as the 10th and 90th percentiles are shown.

As for reliability, we expect a large set of runs of the PS-BB algorithm to produce a somewhat decent sample of all the possible tile sets for a pattern. Based on this, large and small tile sets seem to have a high reliability while medium-size tile sets are clearly less reliable on average. This observation reduces the problem of finding reliable tile sets back to the problem of finding small tile sets. However, it is important to note that artefacts of the algorithm may have an effect on the exact reliability of the tile sets found.

8. Conclusions

We have investigated several algorithmic approaches towards the efficient solution of the PATS problem, i.e., the task of finding minimal tiles sets which would self-assemble into a given k-coloured pattern starting from a bordering seed structure.

Our first algorithm is an exhaustive branch-and-bound method (PS-BB) which, given enough time, explores the entire search space of pattern-consistent tile sets. Numerical experiments indicate that the PS-BB algorithm is able to find minimal tile sets for randomly generated binary patterns of sizes up to 6×6 tiles. However, for larger patterns, the search space becomes too large for a complete exploration, even with the efficient pruning heuristics applied by the algorithm.

In a second approach, we addressed the relaxed objective of generating small but not necessarily minimal tile sets. Here our PS-H algorithm applies heuristic rules for optimising the order in which the search space of pattern-consistent tile sets is explored. Experimental results show that for most patterns, the PS-H algorithm is indeed able to find significantly smaller solutions in a reasonable amount of time than the PS-BB algorithm. Also the reliability of the tile sets produced by the PS-H method clearly exceeds that of the tile sets produced by the PS-BB algorithm.

In a third direction, we also considered solving the PATS problem using logic programming techniques, specifically the Answer Set Programming (ASP) method. For patterns having small minimal solutions, our chosen ASP solver was mostly very successful in discovering these solutions; however the running time of the solver seems to increase rapidly with the size of the minimum solution.

References

[1] J. Clausen and M. Perregaard. On the best search strategy in parallel branch-and-bound: Best-first search versus lazy depth-first search. *Ann. Oper. Research*, 90:1–17, 1999.

[2] E. Czeizler, T. Lempiäinen, and P. Orponen. A design framework for carbon nanotube circuits affixed on DNA origami tiles. In *Proc. 8th Annual Conf. on Foundations of Nanoscience: Self-Assembled Architectures and Devices*, pages 186–187, 2011. Poster.

[3] E. Czeizler and A. Popa. Synthesizing minimal tile sets for complex patterns in the framework of patterned DNA self-assembly. In *Proc. 18th Intl. Conf. on DNA Computing and Molecular Programming*, to appear.

[4] S. M. Douglas, H. Dietz, T. Liedl, B. Hogberg, F. Graf, and W. M. Shih. Self-assembly of dna into nanoscale three-dimensional shapes. *Nature*, 459(7245):414–418, 2009.

[5] K. Fujibayashi, R. Hariadi, S. H. Park, E. Winfree, and S. Murata. Toward reliable algorithmic self-assembly of DNA tiles: a fixed-width cellular automaton pattern. *Nano Letters*, 8:1791–1797, 2008.

[6] K. Fujibayashi and S. Murata. Precise simulation model for DNA tile self-assembly. *IEEE Trans. Nanotechnology*, 8, 2009.

[7] C. P. Gomes and B. Selman. Algorithm portfolios. *Artificial Intelligence*, 126(1–2):43–62, 2001.

[8] M. Göös and P. Orponen. Synthesizing minimal tile sets for patterned DNA self-assembly. In *Proc. 16th Intl. Conf. on DNA Computing and Molecular Programming*, volume 6518 of *LNCS*, pages 71–82. Springer, 2011.

[9] K. N. Kim, K. Sarveswaran, L. Mark, and M. Lieberman. DNA origami as self-assembling circuit boards. In *Proc. 9th Intl. Conf. on Unconventional Computation*, volume 6079 of *LNCS*, pages 56–68. Springer, 2010.

[10] A. Kuzyk, K. T. Laitinen, and P. Törmä. Dna origami as a nanoscale template for protein assembly. *Nanotechnology*, 20(23), 2009.

[11] T. Lempiäinen, E. Czeizler, and P. Orponen. Synthesizing small and reliable tile sets for patterned DNA self-assembly. In *Proc. 17th Intl. Conf. on DNA Computing and Molecular Programming*, volume 6937 of *LNCS*, pages 71–82. Springer, 2011.

[12] J. Li, H. Pei, B. Zhu, L. Liang, M. Wei, Y. He, N. Chen, D. Li, Q. Huang, and C. Fan.

[13] V. Lifschitz. What is answer set programming? In *Proc. 23rd Natl. Conf. on Artificial Intelligence*, volume 3, pages 1594–1597. AAAI Press, 2008.

[14] J. Liu, Z. Cao, and Y. Lu. Functional nucleic acid sensors. *Chem. Rev.*, 109(5):1948–1998, 2009.

[15] W. Liu, H. Zhong, R. Wang, and N. C. Seeman. Crystalline two-dimensional DNA-origami arrays. *Angewandte Chemie International Edition*, 50(1):264–267, 2011.

[16] M. Luby, A. Sinclair, and D. Zuckerman. Optimal speedup of Las Vegas algorithms. *Information Processing Letters*, 47(4):173–180, 1993.

[17] J. S. Lucia, H. T. Allawi, and P. A. Seneviratne. Improved nearest neighbor parameters for predicting DNA duplex stability. *Biochemistry*, 35, 1996.

[18] K. Lund, A. J. Manzo, N. Dabby, N. Michelotti, A. Johnson-Buck, J. Nangreave, S. Taylor, R. Pei, M. N. Stojanovic, N. G. Walter, E. Winfree, and H. Yan. Molecular robots guided by prescriptive landscapes. *Nature*, 465(7295):206–210, 2010.

[19] X. Ma and F. Lombardi. Synthesis of tile sets for DNA self-assembly. *IEEE Trans. on Computer-Aided Design of Integrated Circuits and Systems*, 27:963–967, 2008.

[20] H. T. Maune, S. Han, R. D. Barish, M. Bockrath, W. A. G. III, P. W. K. Rothemund, and E. Winfree. Self-assembly of carbon nanotubes into two-dimensional geometries using DNA origami templates. *Nature Nanotechnology*, 5:61–66, 2010.

[21] S. H. Park, H. Yan, J. H. Reif, T. H. LaBean, and G. Finkelstein. Electronic nanostructures templated on self-assembled DNA scaffolds. *Nanotechnology*, 15:S525–S527, 2004.

[22] L. Qian and E. Winfree. Scaling up digital circuit computation with dna strand displacement cascades. *Science*, 332(6034):1196–1201, 2011.

[23] L. Qian, E. Winfree, and J. Bruck. Neural network computation with dna strand displacement cascades. *Nature*, 475(7356):368–372, 2011.

[24] A. Rajendran, M. Endo, Y. Katsuda, K. Hidaka, and H. Sugiyama. Programmed two-dimensional self-assembly of multiple DNA origami jigsaw pieces. *ACS Nano*, 5(1):665–671, 2011.

[25] P. W. K. Rothemund. Folding DNA to create nanoscale shapes and patterns. *Nature*, 440:297–302, 2006.

[26] P. W. K. Rothemund and E. Winfree. The program-size complexity of self-assembled squares (extended abstract). In *Proc. 32nd Annual ACM Symp. on Theory of Computing*, pages 459–468. ACM, 2000.

[27] R. Schulman and E. Winfree. Programmable control of nucleation for algorithmic self-assembly. *SIAM Journal of Scientific Computing*, 39, 2009.

[28] S. Seki. Combinatorial optimizations in pattern assembly. Manuscript, submitted for publication, 2012.

[29] T. Syrjänen and I. Niemelä. The Smodels system. In *Proc. 6th Intl. Conf. on Logic Programming and Nonmonotonic Reasoning*, volume 2173 of *LNCS*, pages 434–438. Springer, 2001.

[30] E. Winfree. Simulations of Computing by Self-Assembly. Technical Report CSTR 1998.22, California Institute of Technology, 1998.

[31] E. Winfree, F. Liu, L. A. Wenzler, and N. C. Seeman. Design and self-assembly of two-dimensional DNA crystals. *Nature*, 394, 1998.

[32] H. Yan, S. H. Park, G. Finkelstein, J. H. Reif, and T. H. LaBean. DNA-templated self-assembly of protein arrays and highly conducive nanowires. *Science*, 301:1882–1884, 2003.

[33] Z. Zhang, E. M. Olsen, M. Kryger, N. V. Voigt, T. Tørring, E. Gültekin, M. Nielsen, R. MohammadZadegan, E. S. Andersen, M. M. Nielsen, J. Kjems, V. Birkedal, and K. V. Gothelf. A dna tile actuator with eleven discrete states. *Angew. Chem. Int. Ed.*, 50(17):3983–3987, 2011.

Supplementary information

A Design Framework for Carbon Nanotube Circuits Affixed on DNA Origami Tiles

Recent years have witnessed a burst of experimental activity concerning algorithmic self-assembly of nanostructures, motivated at least in part by the potential of this approach as a radically new manufacturing technology. One of the presently most reliable self-assembling, programmable nanostructure architectures is DNA origami [10]. Several authors have announced the formation of DNA origami tiles, capable of further assembly into larger, fully addressable, 1D and 2D scaffolds [3, 5, 8]. Such scaffolds make possible the construction of highly complex structures on top of them [6], prospectively including nanocircuits. In [1], the authors propose a generic framework for the design of Carbon-Nanotube Field Effect Transistor (CNFET) circuits. The elements of these circuits are Carbon Nanotube Field Effect Transistors and Carbon Nanotube Wires. They are placed on top of different DNA origami tiles which self-assemble into any desired circuit.

Single-wall carbon nanotubes (CN's) can be fabricated either metallic (m) or semiconducting (s). A cross-junction between an m- and s-type CN generates a structure with field effect transistor (FET) behavior [2, 7]. In this way, both p-type and n-type FETs are realizable (a p-type FET is ON when input is "0", while an n-type FET is ON when input is "1"). Moreover, experimental implementations have been provided, affixing these structures on top of DNA origami [4, 9].

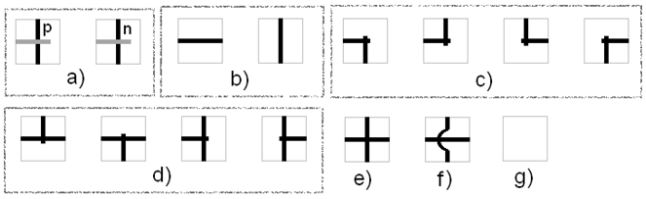

Figure 1: The 14 tile types and the blank tile, out of which any CNFET circuit can be assembled: a) p-type and n-type CNFETs, b) straight CNWs, c) corner CNWs, d)-e) 3- and 4-way CNW junctions, f) crossing but non-interacting CNWs, g) blank tile.

Based on the above experimental results, in [1] the authors provide a "universal" set of 14 functionalised DNA origami tiles, see Figure 1, such as, with a proper selection of "glues" on the tiles, any desired CNFET circuit can be self-assembled from this basis. These tile types are (the marks on the tiles indicate the arrangements of the CNs affixed on the respective DNA origami): a) p-type and n-type CNFETs, b) straight (horizontal or vertical) CN wires (CNWs), c) corner CNWs, d)-e) 3- and 4-way junction CNWs, and f) crossing but non-interacting CNWs. Additionally, when analyzing fault tolerant architectures, it

is convenient to introduce also a blank tile g). In order to design a particular nanocircuit, one first prepares the transistor circuit design using the 14 basis tiles indicated. Then, an optimal number of glues for these tiles is computed and finally, appropriate sticky ends are designed for the DNA origami tiles. In Figure 2 we present the designs for a CMOS Invertor, NAND-gate, and Full Adder, respectively.

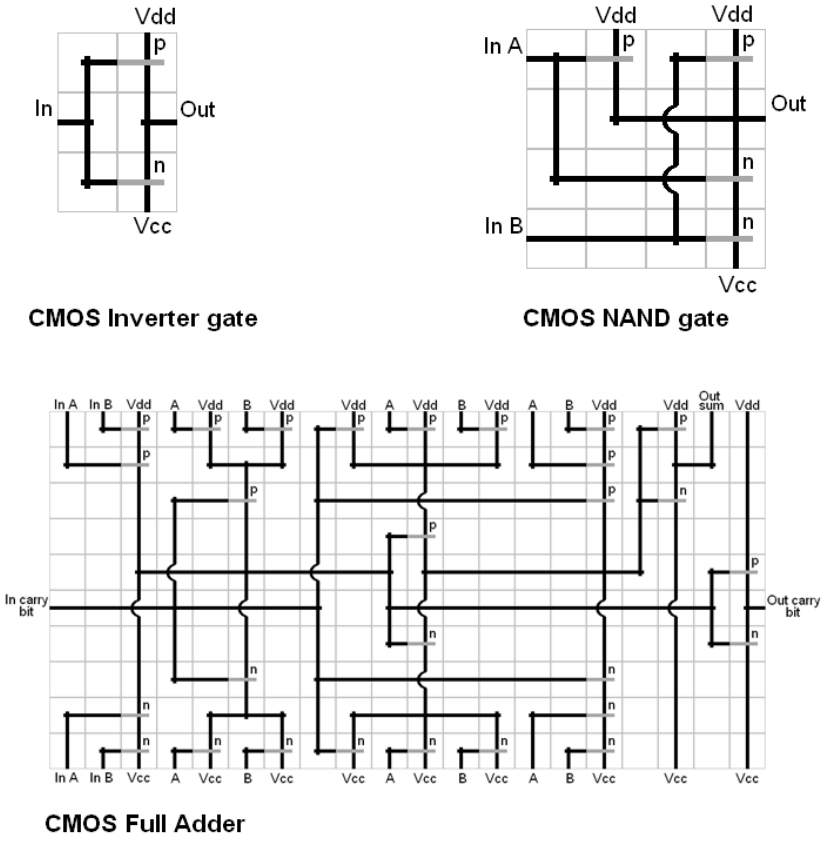

Figure 2: Examples of CNFET circuit design: Invertor gate, NAND gate, and Full Adder.

Some of the advantages of this approach are that it decouples the self-assembly aspects of the manufacturing process from the transistor circuit design and that it allows for a structured and clear circuit design. Moreover, it also supports efficient high-level analysis of the purported circuits, both by computer simulations and by analytical means. For instance, all assembly errors can at this level be treated as tiling errors, leading to a transparent design discipline for fault-tolerant architectures.

References

[1] E. Czeizler, T. Lempiäinen, and P. Orponen. A design framework for carbon nanotube circuits affixed on DNA origami tiles. In *Proc. 8th Annual Conf. on Foundations of Nanoscience: Self-Assembled Architectures and Devices*, pages 186–187, 2011. Poster.

[2] C. Dwyer, V. Johri, M. Cheung, J. Patwardhan, A. Lebeck, and D. Sorin. Design tools for a dna-guided self-assembling carbon nanotube technology. *Nanotechnology*, 15(9), 2004.

[3] M. Endo, T. Sugita, Y. Katsuda, K. Hidaka, and H. Sugiyama. Programmed-assembly system using DNA jigsaw pieces. *Chemistry - A European Journal*, 16(18):5362–5368, 2010.

[4] A.-P. Eskelinen, A. Kuzyk, T. K. Kaltiaisenaho, M. Y. Timmermans, A. G. Nasibulin, E. I. Kauppinen, and P. Törmä.

[5] K. N. Kim, K. Sarveswaran, L. Mark, and M. Lieberman. DNA origami as self-assembling circuit boards. In *Proc. 9th Intl. Conf. on Unconventional Computation*, volume 6079 of *LNCS*, pages 56–68. Springer, 2010.

[6] A. Kuzyk, K. T. Laitinen, and P. Törmä. Dna origami as a nanoscale template for protein assembly. *Nanotechnology*, 20(23), 2009.

[7] Lee, D. Su, Svensson, Johannes, Lee, S. Wook, Park, Y. Woo, Campbell, and E. B. Eleanor. Fabrication of crossed junctions of semiconducting and metallic carbon nanotubes: A CNT-gated CNT-FET. *Journal of Nanoscience and Nanotechnology*, 6(5), 2006.

[8] W. Liu, H. Zhong, R. Wang, and N. C. Seeman. Crystalline two-dimensional DNA-origami arrays. *Angewandte Chemie International Edition*, 50(1):264–267, 2011.

[9] H. T. Maune, S. Han, R. D. Barish, M. Bockrath, W. A. G. III, P. W. K. Rothemund, and E. Winfree. Self-assembly of carbon nanotubes into two-dimensional geometries using DNA origami templates. *Nature Nanotechnology*, 5:61–66, 2010.

[10] P. W. K. Rothemund. Folding DNA to create nanoscale shapes and patterns. *Nature*, 440:297–302, 2006.